ORIGINAL PAPER

Computationally designed prodrugs of statins based on Kirby's enzyme model

Rafik Karaman · Wajd Amly · Laura Scrano · Gennaro Mecca · Sabino A. Bufo

Abstract DFT calculations at B3LYP/6-31G(d,p) for intramolecular proton transfer in Kirby's enzyme models **1**–**7** demonstrated that the reaction rate is dependent on the distance between the two reacting centers, r_{GM}, and the hydrogen bonding angle, α, and the rate of the reaction is linearly correlated with r_{GM} and α. Based on these calculation results three simvastatin prodrugs were designed with the potential to provide simvastatin with higher bioavailability. For example, based on the calculated log EM for the three proposed prodrugs, the interconversion of simvastatin prodrug **ProD 3** to simvastatin is predicted to be about 10 times faster than that of either simvastatin prodrug **ProD 1** or simvastatin **ProD 2**. Hence, the rate by which the prodrug releases the statin drug can be determined according to the structural features of the promoiety (Kirby's enzyme model).

Introduction

Hyperlipidemia is a common heterogeneous group of disorders, most commonly treated with statin medications. Statins

R. Karaman (✉) · W. Amly
Bioorganic Chemistry Department, Faculty of Pharmacy, Al-Quds University, P. O. Box 20002, Jerusalem, Palestine
e-mail: dr_karaman@yahoo.com

R. Karaman · L. Scrano · S. A. Bufo
Department of Sciences, University of Basilicata, Via dell'Ateneo Lucano 10, Potenza 85100, Italy

G. Mecca
Exo Research Organization, Potenza, Italy

are selective and competitive inhibitors of HMG-CoA reductase, the rate-limiting enzyme that converts 3-hydroxy-3-methylglutaryl coenzyme A to mevalonate, a precursor of cholesterol [1]. The chemical structures of statins can be divided into three parts: HMG-CoA substrate analogue; a complex hydrophobic ring structure that is covalently linked to the substrate analogue and is involved in binding of the statin to the reductase enzyme; functional groups on the rings that specify the solubility properties of the drugs and hence their pharmacokinetic properties (see Fig. 1) [2]. Crystal structures of the catalytic portion of the enzyme bound to different statins have revealed that statins bind to the active site of the enzyme sterically preventing the substrate from binding. The substrate-binding pocket of the enzyme also undergoes a rearrangement that allows the rigid, hydrophobic ring molecules of the statins to be accommodated [2]. As a conclusion, an additional hydrogen bond was demonstrated in the atorvastatin–and rosuvastatin–enzyme complexes along with a polar interaction unique to rosuvastatin, such that rosuvastatin has the most binding interactions with HMG-CoA reductase among all the statins [2].

Statins are hepatoselective and the mechanisms contributing to this are governed by the solubility profile of the statin. Passive diffusion through hepatocellular membranes is the key for effective first pass uptake for hydrophobic statins, which can also diffuse to non-hepatocellular parts, whereas extensive carrier-mediated uptake is the major uptake route for hydrophilic statins [2]. This can prove that hydrophilic statins acquire greater hepatoselectivity. All statin are absorbed rapidly after administration, reaching peak plasma concentration within 4 h [2], and all have the liver as their target organ [1]. Statins in general have a low bioavailability mostly due to the extensive first pass effect and/or bad solubility.

Simvastatin is a hydrophobic fungal derivative compound [1]. It is administered as a lactone pro-drug (simvastatin A, Fig. 1) that after oral ingestion undergoes a hydroxylation reaction to yield its corresponding (beta)-hydroxy acid form (simvastatin B,

Fig. 1 Chemical structures for simvastatin, atorvastatin and rosuvastatin

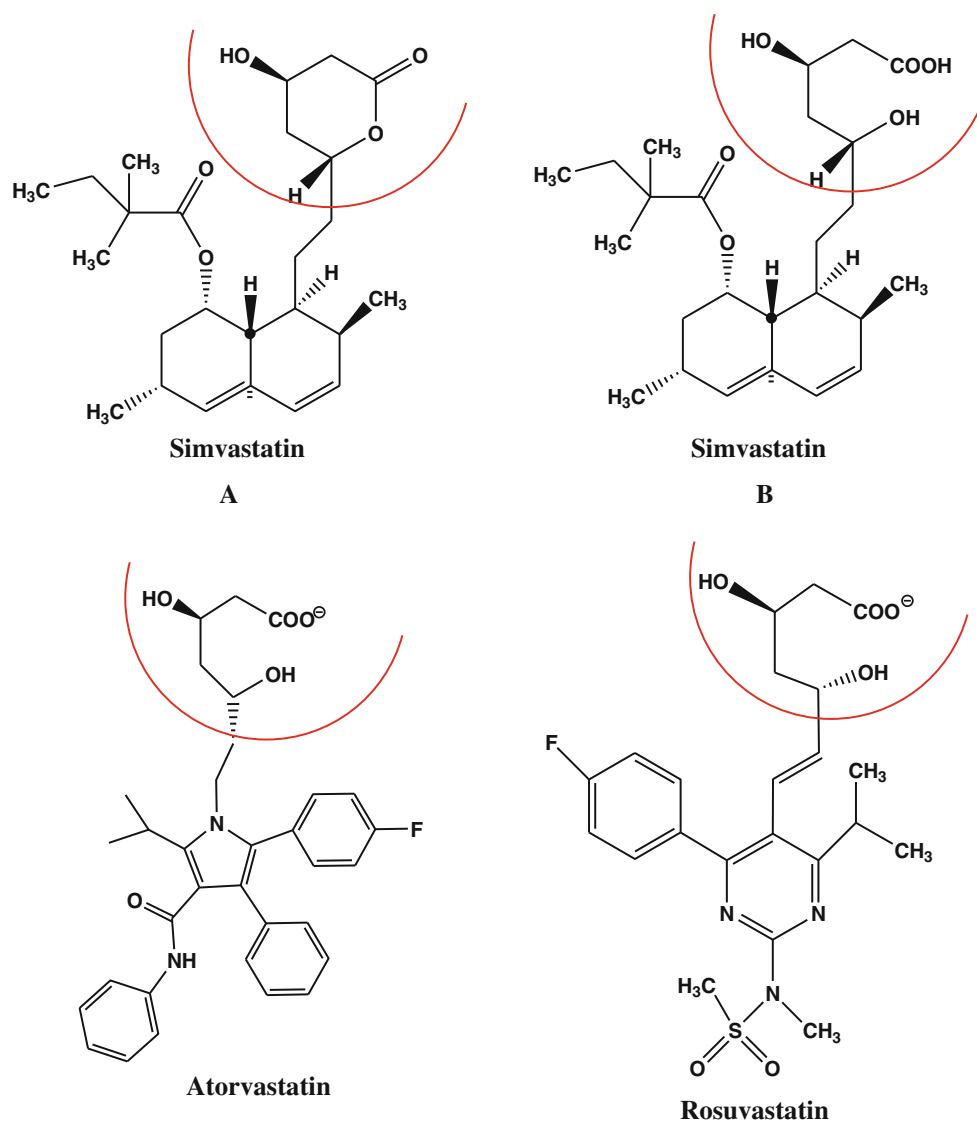Simvastatin A

Simvastatin B

Atorvastatin

Rosuvastatin

Fig. 1) which is an inhibitor of HMG-CoA reductase [3]. The percentage of simvastatin dose retained by the liver is >80 % [1].

The solubility of simvastatin is the limiting factor for its bioavailability [7]. It undergoes an extensive first pass effect and has a bioavailability of only 5 %, it has a poor absorption rate from the gastro-intestinal tract (GIT); therefore, improving its solubility and hence its dissolution rate is a must to enhance its bioavailability [2, 4].

Many attempts have been made in order to improve simvastatin bioavailability. One strategy was by co-solvent evaporation method, where a hydrophilic, low viscosity grade polymer hydroxypropylmethylcellulose (HPMC) was used to enhance the solubility and dissolution of simvastatin. In this method spray drying and rotaevaporation were applied for solvent evaporation. The study results using this method revealed a significant enhancement of simvastatin solubility by converting its regular form to amorphous form via reducing the particle size and increasing wettability [4].

In another study glycerylmonooleate (GMO)/poloxamer 407 cubic nanoparticles was investigated as potential oral drug delivery system to enhance simvastatin bioavailability. The study showed that oral bioavailability of simvastatin cubic nanoparticles was enhanced significantly at 2.41-fold compared to micronized simvastatin crystal powder. In addition, it demonstrated a sustained plasma simvastatin level for over 12 h [6]. Moreover, in 2012, developments of stable pellets-layered simvastatin nano-suspensions were tested for simvastatin dissolution and bioavailabilty. The study revealed that the pellet-layered simvastatin nano-suspensions improved both the dissolution and bioavailability of the drug [3].

Atorvastatin and rosuvastatin (Fig. 1) are fully synthetic compounds. Atorvastatin is relatively lipophilic [1], whereas rosuvastatin is more hydrophilic as a result of a polar hydroxyl group and a methane sulphonamide group, respectively [2]. Atorvastatin has a bioavailability of only 14 %. Its half-life is 14 h, but the half-life of its inhibitory activity for HMG-CoA

reductase is 20 to 30 h due to the contribution of active metabolites. It is extensively metabolized to *ortho-* and *para-*hydroxylated derivatives and various beta-oxidation products, 70 % of circulating inhibitory activity for it is attributed to active metabolites [5].

The problem with atorvastatin is that its instability toward environmental conditions such as heat, moisture or light when packed in any solid dosage form; its hydroxy acid form is converted to the corresponding lactone form [7]. Atorvastatin instability which leads to poor solubility is the main reason for its low bioavailability, as the hepatic first-pass effect is too small to completely explain its low bio-availability; it might be a cause of incomplete intestinal absorption and/or extensive gut wall extraction [7].

One method that was performed in an attempt to improve the oral bioavailability of atorvastatin was by using a stabilized gastro-retentive floating dosage form, where floating formulations usually guarantee a complete, constant release of the drug within a period of 12 h in particular for drugs absorbed in the gastric region, thereby enhancing bioavailability [7].

Different approach was utilizing cyclodextrin complexation to enhance the solubility and stability of atorvastatin, where the in vitro studies showed that the solubility and dissolution rate of atorvastatin- Ca were significantly improved by beta-CD complexation with respect to the drug alone [8].

Rosuvastatin has a bioavailability of about 20 % and is metabolized to its major metabolite; N-desmethyl rosuvastatin, and has approximately one-sixth to one-half the HMG-CoA reductase inhibitory activity of rosuvastatin [3]. In an attempt to improve the medication bioavailabilty, efforts to prepare and optimize microemulsion of rosuvastatin calcium were made, as micro-emulsions are a thermodynamically stable system and can provide higher solubilization. The study demonstrated the potential use of microemulsion system to enhance the solubility and hence bioavailability for the poorly water soluble drug, rosuvastatin [9].

Increasing the utility of biologically active compounds can be accomplished using the prodrug approach strategy, because one can optimize any of the absorption, distribution, metabolism and elimination (ADME) properties of potential drugs to reach a satisfactory bioavailability. Generally, prodrugs contain a linker that is cleaved by an enzymatic or chemical reaction, while other prodrugs release their parent drugs after chemical modification such as an oxidation or reduction reaction. The prodrug candidate can also be synthesized as a double prodrug, where the second linker is attached to the first promoiety linked to the parent drug molecule. These linkers are usually different and are cleaved by different mechanisms. In some cases, two biologically active drugs can be linked together in a single molecule called a codrug. In a codrug, each drug acts as a linker for the other [10, 11].

The presence of many intrinsic and extrinsic factors such as wide interspecies variations in both the expression and function of the major enzyme systems activating prodrugs can affect the conversion process of prodrugs to their parent drugs is considered the most vulnerable link in the chain [12, 13].

In the last 5 years we have been engaged in design of innovative prodrugs with higher bioavailabilities for drugs containing hydroxyl, phenol, or amine group using modern computational methods. For example, mechanisms of several enzyme models that were synthesized to gain a better understanding of enzyme catalysis have been researched and utilized by us for the design of novel prodrug promoiety [14–35]. Using DFT, molecular mechanics and ab initio methods, we have studied different enzyme models for assigning the driving forces that playing dominant roles in governing the reaction rate. Among the enzyme model processes investigated are: (a) proton transfer between two oxygens [36–40] and proton transfer between nitrogen and oxygen in Kirby's enzyme models [36–40]; (b) intramolecular acid-catalyzed hydrolysis in Kirby's maleamic acid amide derivatives [41]; (c) proton transfer between two oxygens in Menger's rigid systems [42–45]; (d) acid-catalyzed lactonization of Cohen's [46–48] and Menger's [42–45] hydroxy-acids; and (e) SN2-based ring-closing reactions as studied by Brown, Bruice, and Mandolini [49–52].

It was demonstrated from our computational studies on intramolecularity [14–35] that there is a need to further investigate the reaction mechanism for determining the factors affecting the reaction rate. This would allow for design of an efficient chemical device that can be used as a prodrug promoiety and that will have the potential to chemically and not enzymatically release the parent drug in a controlled manner. For example, the mechanism for proton transfers in Kirby's enzyme models [36–40] was investigated and directed the synthesis of novel prodrugs of aza-nucleosides for the treatment of myelodysplastic syndromes where the prodrug moiety is linked to one or more of the hydroxyl groups of the nucleoside [53]. The prodrugs were designed such that they undergo interconversion to the corresponding parent drugs in physiological environments, with rates that are solely dependent on the structural features of the pharmacologically inactive promoiety. Different promoiety were also studied for the design of a large number of prodrugs such as anti-Parkinson (dopamine), [54] anti-viral (acyclovir), [55] anti-malarial (atovaquone) [56], anti-hypertensive (atenolol) [57], anti-psoriasis (dimethyl fumarate) [58], decongestant (phenylephrine) [59] and anti-bacterial (cefuroxime) [60] with enhanced dissolution, membrane penetration, and bioavailability. In addition, prodrugs for masking the bitter taste of atenolol, cefuroxime and paracetamol were also designed and synthesized [60–67].

The novel prodrug approach to be discussed in this manuscript implies statins prodrug design based on Kirby's enzyme model [39, 40] (mimicking enzyme catalysis) that has been utilized to understand how enzymes work. The tool

used in the design is a computational approach consisting of calculations using density functional theory (DFT) molecular orbital method and correlations between experimental and calculated values of Kirby's proton transfer processes that were used to understand the mechanism by which enzymes might exert their high rates catalysis. In this approach, no enzyme is needed for the catalysis of the chemical conversion of a prodrug to its active drug. The prodrug conversion rate to the corresponding prodrug is solely dependent on the rate limiting step for the proton transfer reaction.

The solubility of simvastatin is the limiting factor for its bioavailability due to slow tissue penetration [7] hence, it undergoes an extensive first pass effect; therefore, improving its solubility and hence its dissolution rate is a must to enhance its bioavailability. Therefore, development of more hydrophilic prodrugs that have the capability to release the parent drug in physiological environments such as intestine is a significant challenge.

In principle, three approaches could be considered to fulfill the requirements mentioned above: (Fig. 2): (1) linking the statin free hydroxyl group to Kirby's enzyme model (ammonium linker), (2) blocking the statin hydroxyl group with

Kirby's enzyme model (carboxylic acid linker) and (3) attaching the statin free hydroxyl group with Bruice's model (dicarboxylic semi-ester linker).

In this paper, based on proton transfers in Kirby's enzyme models **1**–**7** (Fig. 3) we propose three simvastatin prodrug systems based on proposal 1 shown in Fig. 2.

Based on our reported DFT calculations herein on a proton transfer reaction in some of Kirby's enzyme models, three prodrugs of simvastatin are proposed. As shown in Fig. 4, the simvastatin prodrugs, **ProD 1- ProD 3**, have N, N-dimethylanilinium group (hydrophilic moiety) and a lipophilic moiety (the rest of the prodrug), where the combination of both moieties secures a moderate hydrophilic lipophilic balance (HLB). Furthermore, in a physiological environment of pH around 6, intestine, prodrugs **ProD 1- ProD 3** may have a better bioavailability than their parent drug due to improved absorption. In addition, those prodrugs may be used in different dosage forms (i.e., enteric coated tablets) because of their potential solubility in organic and aqueous media due to the ability of the anilinium group to be converted to the corresponding aniline group in a physiological pH of 6.5.

Fig. 2 Schematic diagram for three proposed approaches to increase statin bioavailability
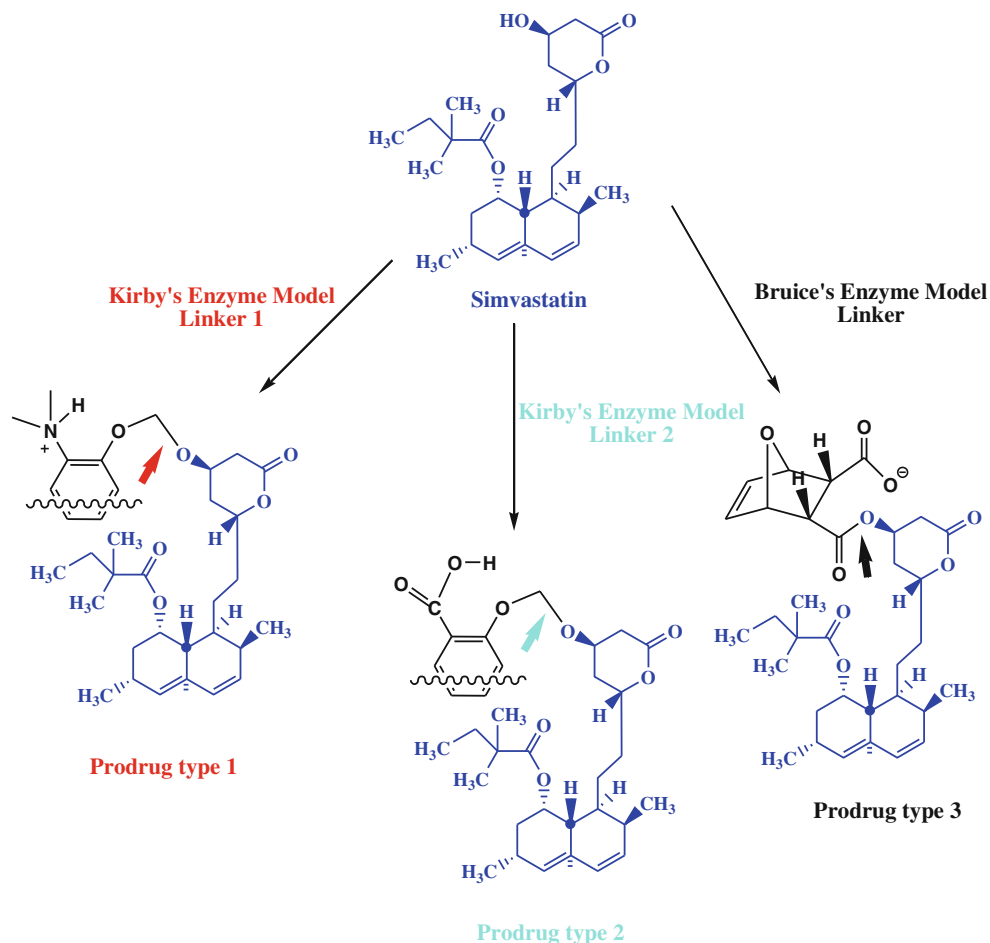
Fig. 3 Proton transfer reactions in systems **1**–**7** and **Inter**

It should be emphasized that at pH 5.5–6.5 (intestine physiological environment) the anilinium form of these pro-drugs will be present mainly as the free aniline form. Only, the former will undergo proton transfer reaction (rate limiting step) to yield the parent drug (simvastatin) and the inactive carrier as a by-product (Fig. 4).

In this paper, we report our DFT study at B3LYP/6-31G(d,p) level of ground state and transition state structures, vibrational frequencies, and reaction trajectories for intramolecular proton transfers in simvastatin prodrugs **ProD 1- ProD 3** (Fig. 4).

Calculations methods

The Becke three-parameter, hybrid functional combined with the Lee, Yang, and Parr correlation functional, denoted B3LYP, were employed in the calculations using density functional theory (DFT). All calculations were carried out using the quantum chemical package Gaussian-2009 [68]. Calculations were carried out based on the restricted Hartree-Fock method [68]. For conservation of computer time, the DFT calculations for simvastatin **ProD 1- ProD 3** were run on

Fig. 4 Interconversion of simvastatin ProD 1- ProD 3 via proton transfer reactions

Simvastatin ProD 1   Linker 1   Simvastatin

Simvastatin ProD 2   Linker 2   Simvastatin

Simvastatin ProD 3   Linker 3   Simvastatin
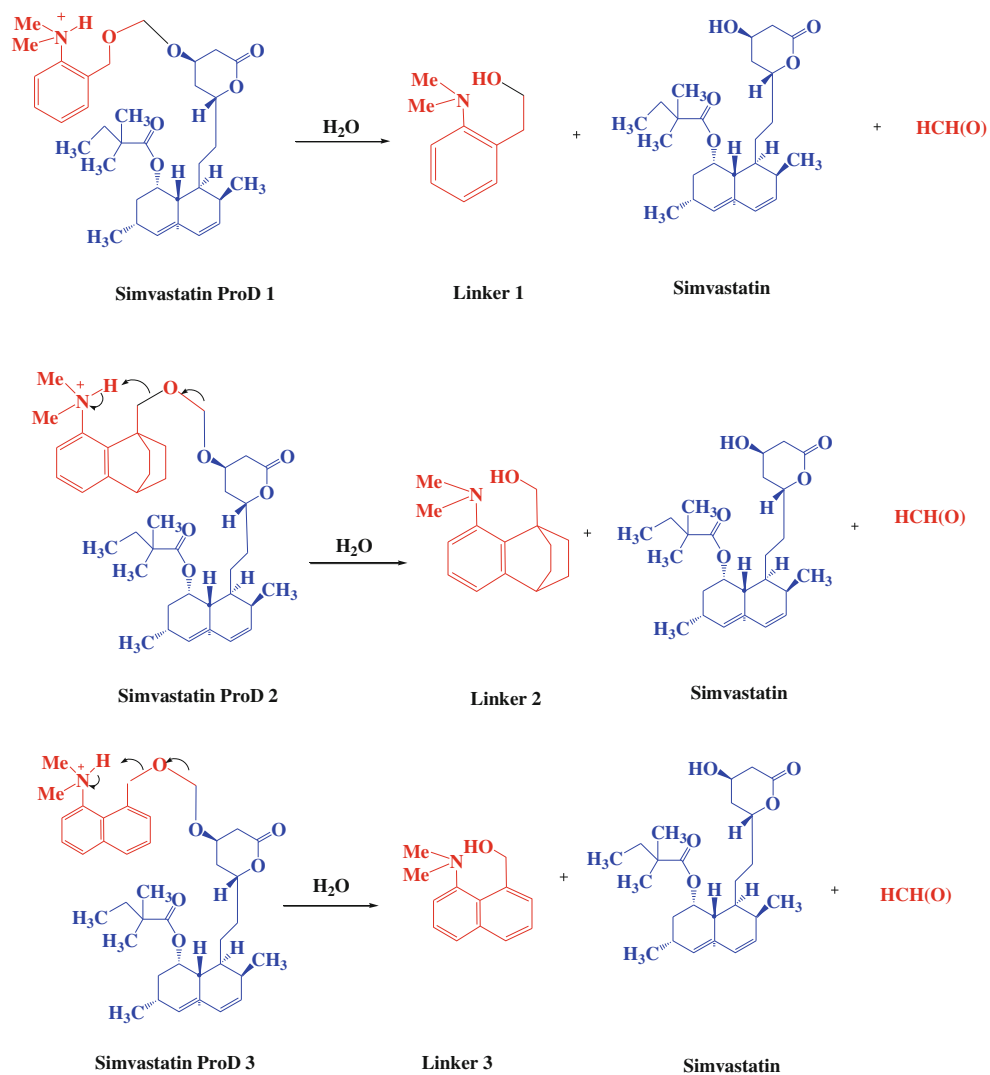
molecules by which the simvastatin structure was represented by the hydroxylactone moiety. It is expected that such

modification will not affect the activation energy values for the entities involved in the proton transfer process. The
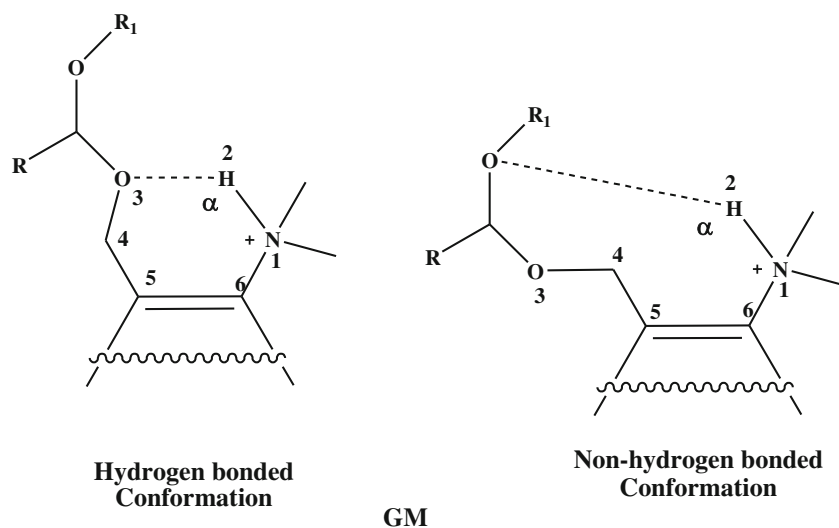

Hydrogen bonded Conformation

Non-hydrogen bonded Conformation

GM

Chart 1 The two possible conformations by which the simvastatin global minimum can exist. α is the angle N1-H2-O3 in the GM
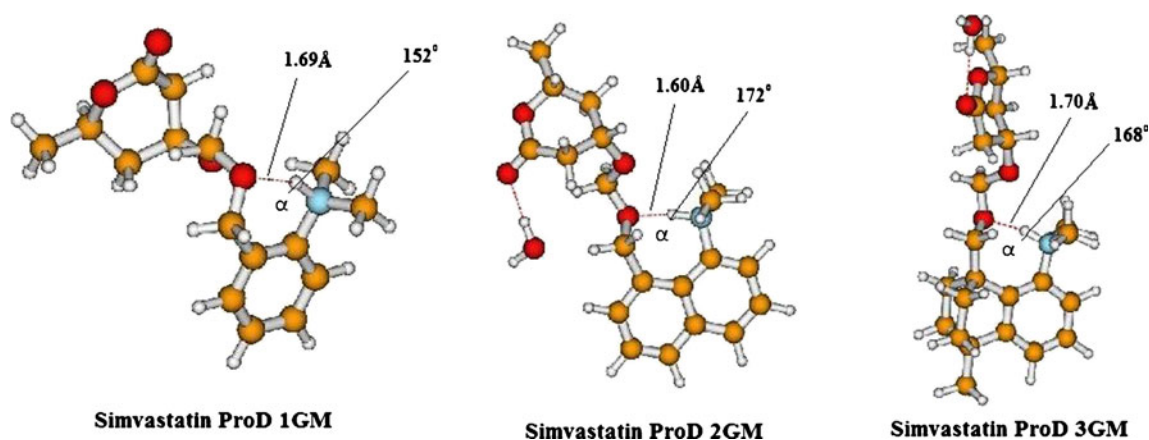
Fig. 5 DFT optimized structures for simvastatin **ProD 1GM**- **ProD 3GM**

starting geometries of all calculated molecules were obtained using the Argus Lab program [69] and were initially optimized with a water molecule at the HF/6-31G level of theory, followed by optimization at the B3LYP/6-31G(d,p) level. Total geometry optimizations included all internal rotations. Second derivatives were estimated for all 3 N-6 geometrical parameters during optimization. The search for the global minimum structure in each of **1**–**7** and simvastatin **ProD1**-**ProD3** was accomplished by 360° rotation of the carboxylic group about the C4-C5 bond (i.e., variation of the dihedral angle O3/C4/C5/C6, Chart 1) in increments of 10° and calculation of the conformational energies (see Chart 1). For systems **1**–**7** and simvastatin prodrugs **ProD 1-ProD 3** two types of conformations in particular were considered: one in which the acetal oxygen is hydrogen bonded with the ammonium hydrogen and another in which it is not. It was found that all global minima exhibit a conformation where the acetal oxygen hydrogen bonded with the ammonium proton (see Chart 1). An energy minimum (a stable compound or a reactive intermediate) has no negative vibrational force constant. A transition state is a saddle point which has only one negative vibrational force constant [70]. Transition states were located first by the normal reaction coordinate method [71] where the enthalpy changes was monitored by stepwise changing the interatomic distance between two specific atoms. The geometry at the highest point on the energy profile was re-optimized by using the energy gradient method at the B3LYP/6-31G(d,p)

level of theory [68]. The "reaction coordinate method" [71] was used to calculate the activation energy in **1**–**7** and simvastatin **ProD1-ProD3** (Figs. 3 and 4). In this method, one bond length is constrained for the appropriate degree of freedom while all other variables are freely optimized. The activation energy values for the proton transfer processes (transfer of H2 from N1 to O3, Chart 1) were calculated from the difference in energies of the global minimum structures (GM) and the derived transition states. Full optimization of the transition states was accomplished after removing any constrains imposed while executing the energy profile. Verification of the desired reactants and products was accomplished using the "intrinsic coordinate method" [71]. The transition state structures were verified by their only one negative frequency. The activation energies obtained from the DFT at B3LYP/6-31G(d, p) level of theory for all molecules were calculated, in the presence of one water molecule.
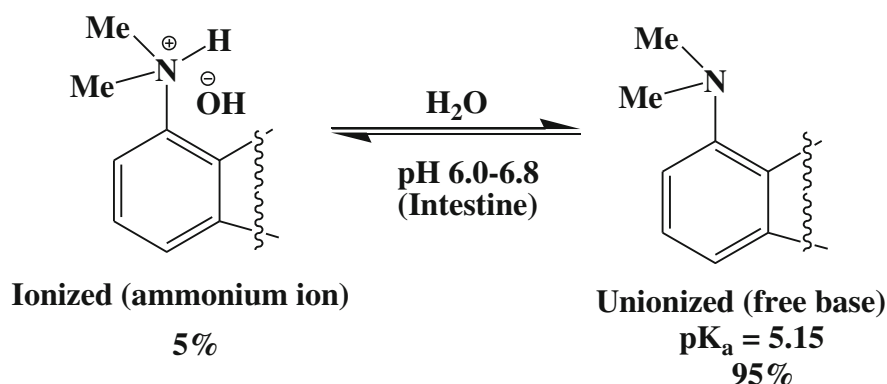
Results and discussion

To provide an efficient pharmacological activity of the statins especially simvastatin (relatively lipophilic system) shown in Fig. 1, the prodrug approach of linking the statin moiety (parent drug) to a relatively hydrophilic (ionized) inactive linker, which upon reaching the physiologic environment,

Table 1 DFT (B3LYP/6-31G(d,p)) calculated properties for the proton transfer reactions in simvastatin **ProD 1-ProD 3**

Structure	DFT enthalpy, H (1H$_2$O) In Hartree	DFT (1H$_2$O) entropy, S, Cal/Mol-Kelvin	DFT (1H$_2$O) frequency Cm^{-1}
SimProD1GM	−1056.0394032	164.31	————
SimProD1TS	−1056.0094695	161.88	1182.99i
SimProD2GM	−1209.6904606	175.75	————
SimProD2TS	−1209.6635091	170.12	1157.05i
SimProD3GM	−1328.834419	198.70	————
SimProD3TS	−1328.8043632	200.11	1149.02i

GM and TS are global minimum and transition state structures, respectively. SimProD refers to simvastatin ProD

releases the parent drug seems to be a promising strategy. The proposed simvastatin prodrugs shown in Fig. 4 are more hydrophilic than the parent drug. Thus enabling the prodrug to penetrate the membrane tissues in much better extent than the parent drug and consequently to prolong the pharmacological activity and to improve the drug therapeutic profile. Kirby's novel study on some enzyme models (ammonium acetals) has inspired us to utilize these systems as potential promoiety (Fig. 3) to statin drugs depicted in Fig. 4. It should be indicated that our proposal is to exploit simvastatin prodrugs **ProD 1- ProD 3** for orally enteric coated tablets use. The physiological environment of the intestine lies in the range of a pH 6.0–6.8. At pH about 6.0 prodrugs **ProD 1- ProD 3** are expected to exist in the unionized (free base) and ionized (ammonium) forms where the equilibrium constant for the exchange between both forms is

dependent on the pK_a of the given prodrug. The experimental pK_a for N,N-dimethylanilinium group is about 5.15 [36–40] hence it is expected that the pK_a values for prodrugs **ProD 1- ProD 3** will be at the same range. Since the pH for the intestine lies in the range around 6.5, the calculated ionized (ammonium)/unionized (free base) ratio will be 1/20 (see Eq. 1). It should be emphasized that the above calculations were based on that **ProD 1- ProD 3** will be absorbed in intestine regions by which the pH is 6.5. However, since the intraluminal pH profile of healthy subjects is rapidly changed from highly acid in the stomach to about pH 6 in the duodenum. The pH gradually increases in the small intestine from pH 6 to about pH 7.4 in the terminal ileum it is expected that the indicated ratio will be changed according to the pH of the physiological part of the GI route.

Ionized (ammonium ion)
5%

H_2O

pH 6.0-6.8
(Intestine)

Unionized (free base)
$pK_a = 5.15$
95%

It is quite safe to assume that both the ionized and unionized forms for prodrugs **ProD 1- ProD 3** (see Eq. 1) will be more hydrophilic than the parent drug due to the presence of the amine (aniline) or ammonium (anilinium) group (Kirby's enzyme model linker). Therefore, the absorption of those prodrugs through the intestinal membranes and the efficiency for delivering the parent drug are expected to be increased.

Our selection of Kirby's enzyme model to be exploited as linkers to simvastatin is based on the fact that these linkers undergo proton transfer reaction to yield an aldehyde, an alcohol and an amine (Fig. 3). The rate-limiting step in these processes, 1–7 (Fig. 3) is a transfer of a proton from the anilinium (ammonium) group into the neighboring acetal oxygen. Furthermore, the proton transfer rate is largely dependent on the hydrogen bonding strength in the products and in the transition states leading to them [36–40]. Hence, it will be safe to predict that the reaction rate will be greatly affected by the structural features of the enzyme model system as evident from the different experimental rate values determined for processes 1–7 [36–40].

Replacing the methoxy group in 1–7 (Fig. 3) with simvastatin drug, as shown for **ProD 1- ProD 3** (Fig. 4) is not expected to have a significant effect on the relative rates of these processes. Therefore, calculations of the kinetic and thermodynamic properties for these enzyme models will shed light on the rates for the chemical intraconversion of simvastatin **ProD 1- ProD 3** to simvastatin.

Conformational analysis for the entities involved
in the proton transfer reactions of Kirby's enzyme models 1–7

Starting structure (reactants, GM) The geometries of the entities involved in the proton transfer reaction of Kirby's enzyme models 1–7 and simvastatin **ProD 1- ProD 3** were calculated in the presence of a water molecule. This is because the experimental proton transfer reaction rates for these processes were determined in aqueous medium. The DFT calculated properties for the reactants of 1–7 (**1GM-7GM**) and simvastatin **ProD 1-ProD 3** (**ProD 1GM- ProD 3GM**) are illustrated in Fig. S1, and Fig. 5 and Table S1 and Table 1, respectively. Careful examination of the calculated structures of **1GM-7GM**

and simvastatin **ProD 1GM**- **ProD 3GM** demonstrates that all geometries except **3GM** and **5GM** exhibit conformation by which the anilinium group is engaged intramolecularly via a hydrogen bonding with the neighboring alkoxy oxygen. This engagement results in the formation of seven-membered ring for simvastatin **ProD 2**- **ProD 3**, six - membered ring for simvastatin **ProD 1**, **1GM**- **2GM**, **4GM** and **6GM** and five-membered ring for **7GM** (see Fig. S1 and Fig. 5). The DFT calculated hydrogen bonding length for the global minimum structures for these processes were 1.60 Å- 2.51 Å and the attack angle α (the hydrogen bond angle, N1H2O3) values range was 107–172°. In addition, it was demonstrated that the hydrogen bonding strength, r_{GM} (H2-O3), is largely dependent on the structural features of the reactant (for the definition of r_{GM} and α see Chart 2). In contrast, no intramolecular hydrogen bond was found in the reactant structures of **3** and **5** (**3GM** and **5 GM**). The distance

r_{GM} (H2-O3) between the ammonium proton and the acetal oxygen in **3GM** and **5 GM** was 3.33 Å (Fig. S1a). The optimized global minimum structures for **3** and **5** were found to be engaged in intermolecular hydrogen bonding with a water molecule.

Transition state structure (TS) The calculated DFT geometrical parameters for the transition state geometries of **1**–**7** (**1TS**-**7TS**) and simvastatin **ProD 1**- **ProD 3**(simvastatin **ProD 1TS**- **ProD 3TS**) are depicted in Fig. S1 and Fig. 6, and Table S1 and Table 1, respectively. Inspection of **1TS**-**7TS** and simvastatin **ProD 1TS**- **ProD 3TS** reveals that all the geometries involve a strong hydrogen bonding between the ammonium proton and the acetal oxygen except **3TS** and **5TS** where they exist in a conformation by which the ammonium and the acetal groups engage intermolecularly in a hydrogen bonding with a molecule of water.
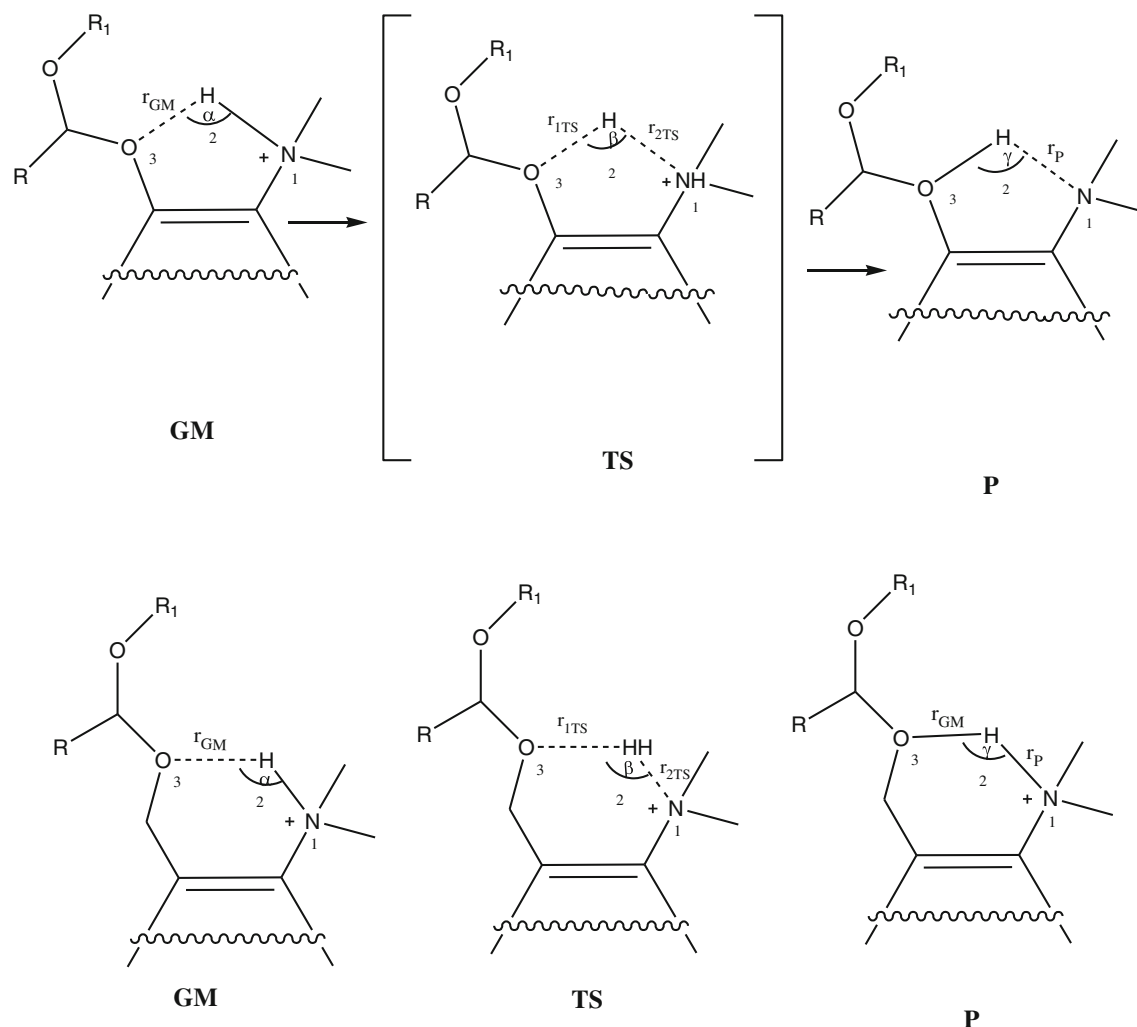

Chart 2 Schematic representation of the proton transfer in Kirby's enzyme models **1**–**7**. GM, TS and P are global minimum, transition state and product structures, respectively. α, β and γ are the angle N1-H2-O3 in the GM, TS and P, respectively. r_{GM}, r_{TS} and r_P are the distances between the two reacting centers in the GM, TS and P, respectively. R is H or phenyl
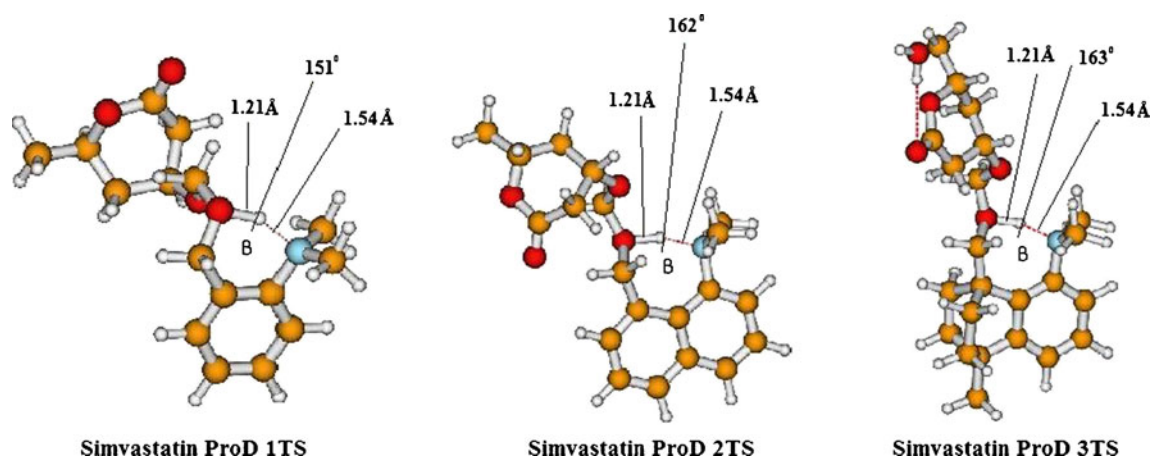
Fig. 6 DFT optimized structures for **ProD 1TS**- **ProD 3TS**

Calculating the proton transfer rate (activation energy, $\Delta G^{\ddagger}$) in Kirby's enzyme models 1–7

Using the quantum chemical package Gaussian-2009 [66] the DFT at B3LYP/6-31G(d,p) level, the enthalpy, entropy and free activation energy values for the proton transfers in processes 1–7 (Fig. 3) and simvastatin **ProD 1**- **ProD 3** were calculated (Fig. 4). The calculated values in the presence of a water molecule are depicted in Table S1 and Table 1, respectively.

Using the calculated DFT enthalpy and entropy energy values for the global minimum structures **1GM-7GM** and simvastatin **ProD 1GM**- **ProD 3GM**, and their derived transition states **1TS-7TS** and simvastatin **ProD 1TS**- **ProD 3TS** (Table S1 and Table 1) the enthalpy ($\Delta H^{\ddagger}$), the entropy ($T\Delta S^{\ddagger}$), and the free activation energy ($\Delta G^{\ddagger}$) values for the proton transfers in these systems were calculated. The calculated values are listed in Table 2.

Mechanistic study for the proton transfer in 1–7 and simvastatin ProD 1- ProD 3

The role of the inter-atomic distance r_{GM} and the attack angle α on the proton transfer rate The DFT calculations for **1GM--7GM** and simvastatin **ProD 1GM- ProD 3GM** demonstrated that these geometries exist in a conformation by which the ammonium proton N1-**H2** engages with the acetal oxygen O3 by a hydrogen bond and the distance r_{GM} (H2-O3) is determined on the structural features of the conformation of the global minimum structure. Low r_{GM} values were obtained when the hydrogen bonding angle (α) value (for a definition, see Chart 2) in the reactants was high and close to 180°, whereas large r_{GM} values were accompanied with small α values (Fig. S1 and Fig. 5, and Table 2). In fact, when r_{GM} was plotted against α linear correlation with a correlation coefficient of $r=0.93$ was obtained.

Table 2 DFT (B3LYP/6-31G(d,p)) calculated kinetic and thermodynamic properties for the proton transfers in **1–7** and simvastatin **ProD1-ProD3** in the presence of one water molecule

System	H2-O3	α	β	$\Delta H^{\ddagger}$	$T\Delta S^{\ddagger}$	$\Delta G^{\ddagger}$	log EM (calc.)
SimProD1	1.69	152	151	18.78	−0.72	19.5	4.64
SimProD2	1.60	172	162	16.91	−1.68	18.59	5.31
SimProD3	1.70	168	163	18.83	0.45	18.38	5.46
1	1.72	146	140	23.62	0.07	23.55	1.67
2	2.04	125	125	24.73	−3.34	28.07	−1.65
3	3.33	123	——	25.41	−4.15	29.56	−2.75
4	1.73	144	145	22.54	0.90	21.64	3.07
5	3.33	124	——	23.59	−4.15	27.74	−1.41
6	1.92	122	122	29.33	0.61	28.72	−2.13
7	2.51	107	133	34.71	−2.00	36.71	−8.01

$\Delta H^{\ddagger}$ is the activation enthalpic energy (kcal mol^{-1}). $T\Delta S^{\ddagger}$ is the activation entropic energy in kcal mol^{-1}

$\Delta G^{\ddagger}$ is the activation free energy (kcal mol^{-1}). α is the hydrogen bonding angle in the ground state structure (see Chart 1). β is the hydrogen bonding angle in the ground state structure (see Chart 1). EM = $e^{-(\Delta G^{\ddagger}_{inter} - \Delta G^{\ddagger}_{intra})/RT}$

Furthermore, Table 2 demonstrates that the enthalpy activation ($\Delta H^{\ddagger}$) and free activation energies ($\Delta G^{\ddagger}$) needed to transfer a proton in systems **1–7** and simvastatin **ProD 1-ProD 3** is significantly affected by the distance r_{GM} (H2-O3), and the hydrogen bonding angle α (N1H2O3) (for the definition for these parameters, see Chart 2). Systems with global minimum structures having low r_{GM} and high α values such as simvastatin **ProD** 1- **ProD 3** and **4**, exhibit higher rates (lower $\Delta G^{\ddagger}$) than those having high r_{GM} and low α values, such as **3** and **7**. When the rGM and α values were examined for correlation with the calculated DFT free activation ($\Delta G^{\ddagger}$) and enthalpy activation energies ($\Delta H^{\ddagger}$) strong correlation with high correlation coefficients, r=0.95–1.0 and 0.90–0.95, respectively, was obtained (Fig. 7a-c).

Calculating the effective molarities (EM) in Kirby's enzyme models 1–7 and simvastatin ProD 1- ProD 3:

The effective molarity (EM) is a parameter used to indicate the efficiency of an intramolecular process and it is defined as the rate ratio k_{intra}/k_{inter} for intramolecular and corresponding intermolecular processes driven by identical mechanisms [72]. Because the EM values for some of the processes shown in Fig. 3 were not experimentally determined we sought to introduce our computational rational for calculating these values based on the calculated DFT activation energies ($\Delta G^{\ddagger}$) for **1–7** and simvastatin **ProD 1-ProD 3** on one hand and the corresponding intermolecular process (**Inter**, Fig. 3) on the other hand. Process **Inter** (Fig. 3) was selected to represent the corresponding intermolecular process for **1–7** and simvastatin **ProD 1-ProD 3**.

Equation 6 that was derived from Eqs. 2–5 describes the EM parameter as a function of the difference in the activation energies of the intra- and the corresponding inter-molecular processes. The EM values for processes **1–7** and simvastatin **ProD 1- ProD 3** depicted in Table 2 were calculated using Eq. 6.

$$EM = k_{intra}\big/ k_{inter} \tag{2}$$

$$\Delta G^{\ddagger}_{intra} = -RT \ln k_{intra} \tag{3}$$

$$\Delta G^{\ddagger}_{inter} = -RT \ln k_{inter} \tag{4}$$

$$\Delta G^{\ddagger}_{intra} - \Delta G^{\ddagger}_{inter} = -RT \ln k_{intra}\big/ k_{inter} \tag{5}$$

$$EM = e^{-(\Delta G^{\ddagger}inter - \Delta G^{\ddagger}intra)\big/ RT} \tag{6}$$

T is 298° K and R is the gas constant.

The calculated EM values for 1–7 and simvastatin **ProD 1- ProD 3** were correlated with the enthalpy ($\Delta H^{\ddagger}$) and free activation ($\Delta G^{\ddagger}$) energies. The correlation results along with the correlation coefficients are illustrated in Fig. 7d. Examination of the EM values shown in Table 2 and Fig. 7d revealed that simvastatin **ProD 1 – ProD 3** are the most efficient processes among all processes (log EM=4.6–5.5) and process 7 is the least with log EM <−8. Although the EM values for 1–7 were not experimentally determined, Kirby and coworkers estimated the experimental log EM value for process **1** in the order of 3 [39, 40]. The calculated EM value for **1** is 1.67. This is in agreement with the corresponding experimental estimated value.

Conclusions

The DFT calculations demonstrate that the rate-limiting step in processes **1–7** and simvastatin **ProD 1- ProD 3** is a transfer of a proton from the ammonium moiety to the acetal oxygen and the reaction rate is largely responsive to geometric disposition, especially to distance between the two reacting centers, r_{GM}, and the hydrogen bonding angle, α. The vital requirement for a system for achieving a high intramolecular proton transfer rate is a short distance between the two reactive centers (r_{GM}) in the ground states (GM) which subsequently results in strong intramolecular hydrogen bonding in the products and the transition states leading to them.

Therefore, we conclude that the our study results reported herein can provide a stepping stone for a design of prodrug systems that can be pharmaceutically used as devices for an efficient slow release of statins in general and simvastatin in particular. For example, based on the calculated log EM, the cleavage process for simvastatin **ProD 2** and simvastatin **ProD 3** may be predicted to be about ten times faster than that for simvastatin **ProD 1**. Hence, the rate by which the prodrug releases the statin drug can be determined according to the structural features of Kirby's enzyme model (the prodrug promoiety).

Our future directions include the synthesis of simvastatin **ProD 1** -**ProD 3** followed by in vitro kinetic studies at different pH values, especially pH 6.5 (intestine environment). The in vitro kinetic data will provide the data basis for the
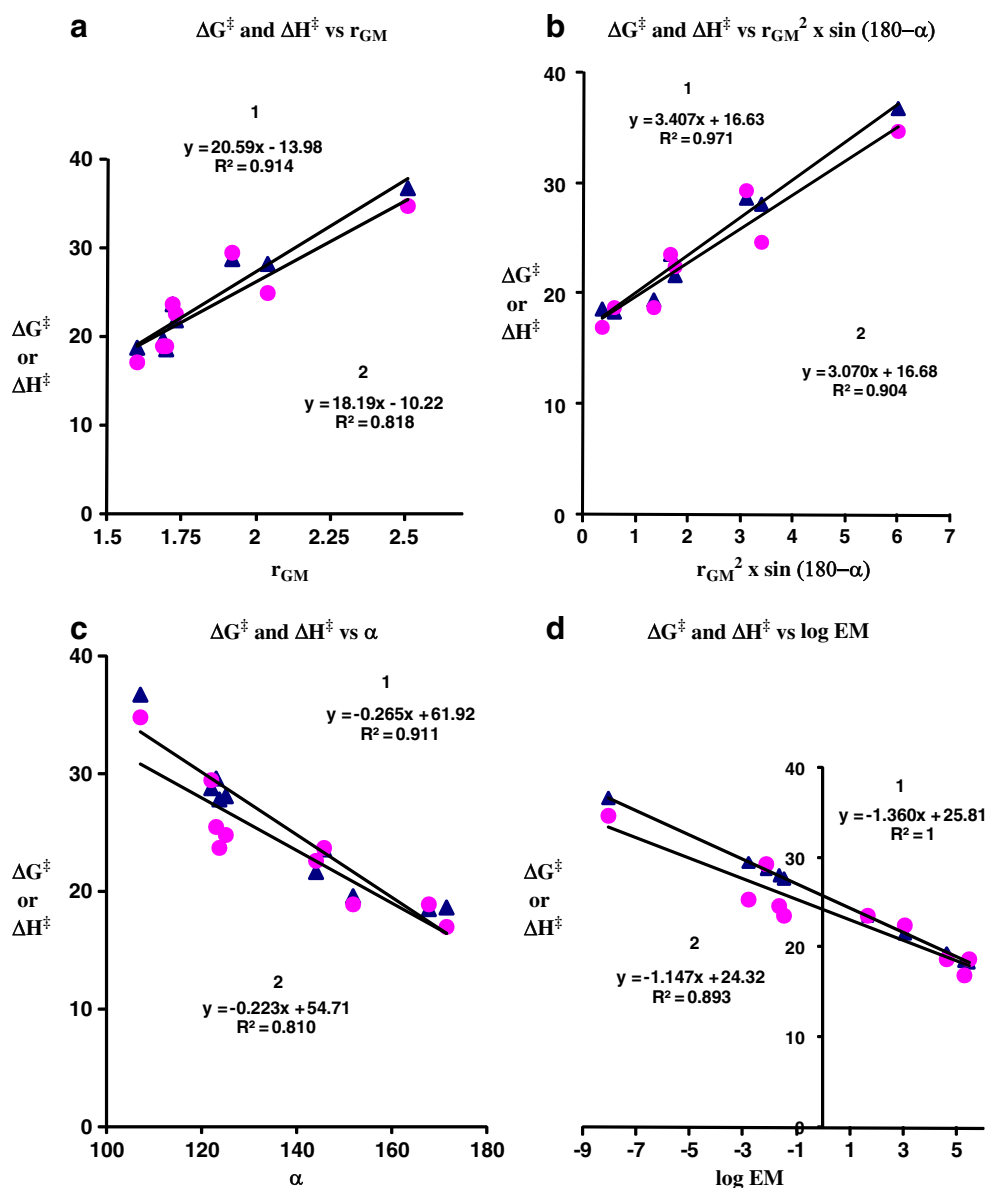
Fig. 7 a Plot of the DFT calculated $\Delta G^{\ddagger}$ and $\Delta H^{\ddagger}$ vs. r_{GM} in **1–7** and simvastatin **ProD 1- ProD 3**, where r_{GM} is the distance between the two reacting centers in the GM structure. **b** Plot of the DFT calculated $\Delta G^{\ddagger}$ and $\Delta H^{\ddagger}$ vs. r_{GM}^{2} x sin (180-α) in **1–7** and simvastatin **ProD 1- ProD 3**, where r_{GM} is the distance between the two reactive centers. **c** Plot of the DFT calculated $\Delta G^{\ddagger}$ and $\Delta H^{\ddagger}$ vs. the hydrogen bonding α (degree) in the GM structures of **1–7** and simvastatin **ProD 1- ProD 3**. **d** Plot of the DFT calculated $\Delta G^{\ddagger}$ and $\Delta H^{\ddagger}$ vs. log EM in **1–7** and simvastatin **ProD 1- ProD 3**, where EM is the calculated effective molarity (see text). Number 1 refers to plots with blue triangle points that represent $\Delta G^{\ddagger}$ in the y-axis and number 2 refers to plots with pink circles that represent $\Delta H^{\ddagger}$ in the y-axis. $\Delta G^{\ddagger}$ and $\Delta H^{\ddagger}$ are in kcal mol^{-1}. r_{GM} is in Å and α in degrees. **Supporting data**: Table S1, Fig. S1 and xyz Cartesian co-ordinates for the DFT optimized GM and TS structures in processes simvastatin **ProD1-ProD 3**

pharmacokinetic studies, in vivo. Based on the in vitro results, one or more of the prodrug systems will be tested in vivo in addition to simvastatin drug as a control. The prodrug will be administered to animals by oral enteric coated tablets, blood and urine samples will be collected at different times. The concentration of the statin will be determined using a reliable bioanalytical method. Further, pharmacokinetic parameter values will be calculated including oral bioavailability, terminal elimination half-life and other pharmacokinetic parameters as deemed necessary.

References

1. Stancu C, Sima A (2001) Statins: mechanism of action and effects. J Cell Mol Med 5(4):378–387

2. Schachter M (2005) Chemical, pharmacokinetic and pharmacodynamic properties of statins: an update. Fundam Clin Pharmacol 19(1):117–125

3. Luo Y, Xu L, Tao X, Xu M, Feng J, Tang X. (2012) Characterization, stability and in vitro-in vivo evaluation of pellet-layered Simvastatin nanosuspensions. Drug Dev Ind Pharm 39(7):936-46 doi:10.3109/03639045.2012.699067

4. Pandya P, Gattani S, Jain P, Khirwal L, Surana S (2008) Co-solvent evaporation method for enhancement of solubility and dissolution rate of poorly aqueous soluble drug simvastatin: in vitro–in vivo evaluation. AAPS Pharm Sci Tech 9(4):1247–1257

5. http://www.theodora.com/drugs/

6. Lai J, Chen J, Lu Y, Sun J, Hu F, Yin Z, Wu W. (2009) Glyceryl monooleate/poloxamer 407 cubic nanoparticles as oral drug delivery systems: I. In nitro evaluation and enhanced oral bioavailability of the poorly water-soluble drug Simvastatin. AAPS Pharm Sci Tech 10(3)::960-966

7. Khan FN, Dehghan MHG (2011) Enhanced bioavailability of atorvastatin calcium from stabilized gastric resident formulation. AAPS Pharm Sci Tech 12(4):1077–1086

8. Palem CR, Patel S, Pokharkar VB (2009) Solubility and stability enhancement of atorvastatin by cyclodextrin complexation. PDA J Pharm Sci Technol 63(3):217–225

9. Patel ZB, Patel KS, Shah AS Surti NI (2012) Preparation and optimization of microemulsion of Rosuvastatin calcium. J Pharm Bioallied Sci 4(Suppl 1):S118–S119

10. Huttunen KM, Raunio H, Rautio J (2011) Prodrugs – from serendipity to rational design. Pharmacol Rev 63:750–771

11. Stella VJ, Nti-Addae KW (2007) Prodrug strategies to overcome poor water solubility. Adv Drug Deliv Rev 59:677–694

12. Gonzalez FJ, Tukey RH (2006) Drug metabolism. In: Brunton LL, Lazo JS, Parker KL (eds) Goodman and Gilman's the pharmacological basis of therapeutics. The McGraw-Hill Companies, Inc. New York, pp 71–91

13. Testa B, Krämer SD (2007) The biochemistry of drug metabolism–an introduction: part 2. Redox reactions and their enzymes. Chem Biodivers 4:257–405

14. Karaman R (2008) Analysis of Menger's spatiotemporal hypothesis. Tetrahedron Lett 49:5998–6002

15. Karaman R (2009) Cleavage of Menger's aliphatic amide: a model for peptidase enzyme solely explained by proximity orientation in intramolecular proton transfer. J Mol Struct (THEOCHEM) 910:27–33

16. Karaman R (2010) The efficiency of proton transfer in Kirby's enzyme model, a computational approach. Tetrahedron Lett 51:2130–2135

17. Karaman R, Pascal RA (2010) Computational analysis of intramolecularity in proton transfer reactions. Org & Bimol Chem 8:5174–5178

18. Karaman R (2010) A general equation correlating intramolecular rates with attack Parameters: distance and angle. Tetrahedron Lett 51:5185–5190

19. Karaman R (2011) Analyzing the efficiency of proton transfer to carbon in Kirby's enzyme model- a computational approach. Tetrahedron Lett 52:699–704

20. Karaman R (2011) Analyzing the efficiency in intramolecular amide hydrolysis of Kirby's N-alkylmaleamic acids - A computational approach. Comput Theor Chem 974:133–142

21. Karaman R (2009) A new mathematical equation relating activation energy to bond angle and distance: A key for understanding the role of acceleration in lactonization of the trimethyl lock system. Bioorganic Chemistry 37:11–25

22. Karaman R (2009) Revaluation of Bruice's proximity orientation. Tetrahedron Lett 50:452–458

23. Karaman R (2009) Accelerations in the lactonization of trimethyl lock systems are due to proximity orientation and not to strain effects. Research Letters in Org Chem. doi:10.1155/2009/240253

24. Karaman R (2009) The *gem*-disubstituent effect- a computational study that exposes the relevance of existing theoretical models. Tetrahedron Lett 50:6083–6087

25. Karaman R (2009) Analyzing Kirby's amine olefin – a model for amino-acid ammonia lyases. Tetrahedron Lett 50:7304–7309

26. Karaman R (2009) The Effective Molarity (EM) puzzle in proton transfer reactions. Bioorganic Chemistry 37:106–110

27. Karaman R (2010) Effects of substitution on the effective molarity (EM) for five membered ring-closure reactions- a computational approach. J Mol Struct (THEOCHEM) 939:69–74

28. Karaman R (2010) The Effective Molarity (EM) Puzzle in intramolecular ring-closing reactions. J Mol Struct (THEOCHEM) 940:70–75

29. Menger FM, Karaman R (2010) A Singularity model for chemicalreactivity. Eur J Chem 16:1420–1427

30. Karaman R (2010) The Effective Molarity (EM) – a computational approach. Bioorganic Chemistry 38:165–172

31. Karaman R (2010) Proximity vs strain in ring-closing reactions of bifunctional chain molecules- a computational approach. J Mol Phys 108:1723–1730

32. Karaman R (2011) The role of proximity orientation in intramolecular proton transfer reactions. J Comput Theor Chem 966:311–321

33. Karaman R, Menger FM (2012) Proton shuffling in acid/base catalyzed enolizations. A computational study. J Phys Org Chem 25:1336–1342

34. Karaman R (2011) Analyzing the efficiency in intramolecular amide hydrolysis of Kirby's N-alkylmaleamic acids - a computational approach. J Comput Theor Chem 974:133–142

35. Karaman R (2012) Computationally designed enzyme models to replace natural enzymes in prodrug approaches. J Drug Design 1:e111. doi:10.4172/2169-0138.1000e111

36. Kirby AJ, Parkinson A (1994) Most efficient intramolecular general acid catalysis of acetal hydrolysis by the carboxyl group. J Chem Soc Chem Commun 707–708

37. Brown CJ, Kirby AJ (1997) Efficiency of proton transfer catalysis. Intramolecular general acid catalysis of the hydrolysis of dialkyl acetals of benzaldehyde. J Chem Soc, Perkin Trans 2:1081–1094

38. Craze G-A, Kirby AJ (1974) The role of the carboxy-group in intramolecular catalysis of acetal hydrolysis. The hydrolysis of substituted 2- methoxymethoxybenzoic acids. J Chem Soc, Perkin Trans 2:61–66

39. Hartwell E, Hodgson DRW, Kirby AJ (2000) Exploring the limits of efficiency of proton-transfer catalysis in models and enzymes. J Am Chem Soc 122:9326–9327

40. Kirby AJ (1997) Efficiency of proton transfer catalysis in models and enzymes. Acc Chem Res 30:290–296

41. Kirby AJ, Lancaster PW (1972) Structure and efficiency in intramolecular and enzymatic catalysis. Catalysis of amide hydrolysis

by the carboxy-group of substituted maleamic acids. J Chem Soc, Perkin Trans 2:1206–1214

42. Menger FM, Ladika M (1988) Fast hydrolysis of an aliphatic amide at neutral pH and ambient temperature. A peptidase model J Am Chem Soc 110:6794–6796

43. Menger FM (1985) On the source of intramolecular and enzymatic reactivity. Acc Chem Res 18:128–134

44. Menger FM, Chow JF, Kaiserman H, Vasquez PC (1983) Directionality of proton transfer in solution. Three systems of known angularity. J Am Chem Soc 105:4996–5002

45. Menger FM, Galloway AL, Musaev DG (2003) Relationship between rate and distance. Chem Commun 2370–2371

46. Milstein S, Cohen LA (1970) Concurrent general-acid and general-base catalysis of esterification. J Am Chem Soc 92:4377–4382

47. Milstein S, Cohen LA (1970) Rate acceleration by stereopopulation control: models for enzyme action. Proc Natl Acad Sci USA 67:1143–1147

48. Milstein S, Cohen LA (1972) Stereopopulation control I. Rate enhancement in the lactonizations of o-hydroxyhydrocinnamic acids. J Am Chem Soc 94:9158–9165

49. Brown RF, van Gulick NM (1956) The geminal alkyl effect on the rates of ring closure of bromobutylamines. J Org Chem 21:1046–1049

50. Bruice TC, Pandit UK (1960) The effect of geminal substitution ring size and rotamer distribution on the intra molecular nucleophilic catalysis of the hydrolysis of monophenyl esters of dibasic acids and the solvolysis of the intermediate anhydrides. J Am Chem Soc 82:5858–5865

51. Bruice TC, Pandit UK (1960) Intramolecular models depicting the kinetic importance of "fit" in enzymatic catalysis. Proc Natl Acad Sci USA 46:402–404

52. Galli C, Mandolini L (2000) The role of ring strain on the ease of ring closure of bifunctional chain molecules. Eur J Org Chem 3117–3125

53. Karaman R (2010) Prodrugs of aza nucleosides based on proton transfer reactions. J Comput Aided Mol Des 24:961–970

54. Karaman R (2011) Computational aided design for dopamine prodrugs based on novel chemical approach. Chem Biol Drug Des 78:853–863

55. Karaman R, Dajani KK, Qtait A, Khamis M (2012) Prodrugs of acyclovir - a computational approach. Chem Biol Drug Des 79:819–834

56. Karaman R, Hallak H (2010) Computer-assisted design of pro-drugs for antimalarial atovaquone. Chem Biol Drug Des 76:350–360

57. Karaman R, Dajani KK, Hallak H (2012) Computer-assisted design for atenolol prodrugs for the use in aqueous formulations. J Mol Model 18:1523–1540

58. Karaman R, Dokmak G, Bader M, Hallak H, Khamis M, Scrano L, Bufo SA (2013) Prodrugs of fumarate esters for the treatment of psoriasis and multiple sclerosis (MS)- a computational approach. J Mol Model 19:439–452

59. Karaman R, Karaman D, Zeiadeh I (2013) Prodrugs for masking bitter taste of antibacterial drugs - a computational approach. J Mol Physics. doi:10.1080/00268976.2013.779395

60. Karaman R (2013) Prodrugs for masking bitter taste of antibacterial drugs - a computational approach. J Mol Model 19:2399–2412

61. Hejaz H, Karaman R, Khamis M (2012) Computer-assisted design for paracetamol masking bitter taste prodrugs. J Mol Model 18:103–114

62. Karaman R (2012) The future of prodrugs designed by computational chemistry. J Drug Design 1:e103. doi:10.4172/ddo.1000e103

63. Dahan A, Khamis M, Agbaria R, Karaman R (2012) Targeted prodrugs in oral drug delivery: the modern molecular biopharmaceutical approach. Expert Opinion on Drug Delivery 9:1001–1013

64. Karaman R (2012) Computationally designed prodrugs for masking the bitter taste of drugs. J Drug Design 1:e106. doi:10.4172/2169-0138.1000e106

65. Karaman R (2013) Prodrugs design by computation methods- a new era. J Drug Design 2:e113. doi:10.4172/2169-0138.1000e113

66. Karaman R (2013) Prodrug design vs. drug design. J Drug Design 2:e114. doi:10.4172/2169-0138.1000e114

67. Karaman R (2013) Prodrugs for masking bitter taste of antibacterial drugs - a computational approach. J Mol Mod 19:2399–2412

68. Gaussian 09, Revision A.1, Frisch MJ, Trucks GW, Schlegel H B. Scuseria GE, Robb MA, Cheeseman JR, Scalmani G, Barone V, Mennucci B, Petersson GA, Nakatsuji H, Caricato M, Li X, Hratchian, H, Izmaylov A F, Bloino J, Zheng G, Sonnenberg JL, Hada M, Ehara M, Toyota K, Fukuda R, Hasegawa J, Ishida M, Nakajima T, Honda Y, Kitao O, Nakai H, Vreven T, Montgomery Jr. JA, Peralta JE, Ogliaro F, Bearpark M, Heyd JJ, Brothers E, Kudin KN, Staroverov VN, Kobayashi R, Normand J, Raghavachari K, Rendell A, Burant JC, Iyengar SS, Tomasi J, Cossi M, Rega N, Millam JM, Klene M, Knox JE, Cross JB, Bakken V, Adamo C, Jaramillo J, Gomperts R, Stratmann RE, Yazyev O, Austin AJ, Cammi R, Pomelli C, Ochterski JW, Martin RL, Morokuma K, Zakrzewski VG, Voth G A, Salvador P, Dannenberg JJ, Dapprich S, Daniels AD, Farkas Ö, Foresman JB, Ortiz JV, Cioslowski J, Fox DJ (2009) Gaussian Inc, Wallingford, CT

69. Casewit CJ, Colwell KS, Rappe AK (1992) Application of a universal force field to main group compounds. J Am Chem Soc 114:10046–10053

70. Murrell JN, Laidler KJ (1968) Symmetries of activated complexes. Trans Faraday Soc 64:371–377

71. Muller K (1980) Reaction paths on multidimensional energy hypersurfaces. Angew Chem Int Ed Engl 19:1–13

72. Kirby AJ (1980) effective molarities for intramolecular reactions. Adv Phys Org Chem 17:183, and references therein